Chapter 4

OPTIMIZATION OF THE ANTENNA

In the last chapter, three types of the rectangular-cavity-backed slot antennas (a single square loop slot antenna, a two-element square loop slot antenna and a two-arm square spiral slot antenna) have been investigated. The discussion concentrated on the realization of circularly polarized waves and the way of enhancing the radiation characteristics. Whereas, the bandwidths of both VSWR and axial ratio have not been optimized.

In this chapter, I will concentrate on the optimization of this kind of antennas and a rectangular-cavity-backed two-element rectangular loop slot antenna for circular polarization is presented and investigated. Two short-circuiting points are introduced on the slots to get circular polarization and a symmetrical radiation pattern.

4.1 Rectangular-Cavity-Backed Two-Element Rectangular Loop Slot Antenna

One annular slot with one short-circuiting point has a shifted radiation pattern maximum of 5–10 degrees from the zenith, due to its unsymmetrical configuration [20]. One rectangular loop slot also has the shifted radiation pattern maximum as discussed in the last chapter (see Fig. 3.11).

In this chapter, a rectangular-cavity-backed two-element rectangular loop slot antenna is proposed to radiate circularly polarized waves and in addition, to get the radiation pattern maximum in the zenith. Two short-circuiting points are set at the symmetrical positions with respect to the center of the structure on the slot to get circular polarization and a symmetrical radiation pattern.

The magnetic current considering the effect of the cavity is obtained for a thin rectangular loop slot and is used to calculate the input impedance, VSWR, radiation pattern, and axial ratio (AR). The calculated results in this chapter are based on the formulation derived in Chapter 2. The calculations of magnetic current and input impedance are according to Eqs. (2.18) and (2.30) of Chapter 2. VSWR and axial ratio (AR) are calculated by using Eqs. (A.5) and (A.21) of Appendix.

The effect of the structural dimensions on the antenna characteristics is discussed, the optimization of the antenna is performed on both AR and VSWR characteristics, and the relevant experiment is conducted to validate the analysis.

4.2 Antenna Structure

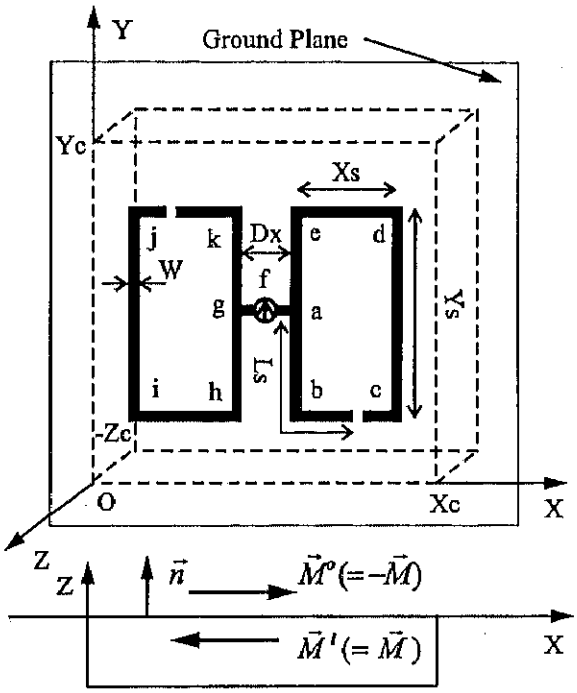

Fig. 4.1: A rectangular-cavity-backed two-element rectangular loop slot antenna.

The model considered and the coordinate system are shown in Fig. 4.1. The two-element rectangular loop slot is placed at the center of the cavity on the ground plane. Dx is the distance between the two rectangular loop slots. Xs and Ys are the length and the width of the rectangular loop slot, respectively. A constant current i_0 is fed across the center of the two-element rectangular loop slot at (Xc/2, Yc/2, 0). To obtain a symmetric traveling wave magnetic current distribution, two short-circuiting points where $\vec{M} = 0$ are set at the two positions (Ls) symmetric to the center of the slot (i.e. the feed point). By adjusting the short-circuiting positions, the circularly polarized waves will be produced by this traveling wave magnetic current.

4.3 Numerical Results

In the calculation, it is assumed that the cavity is a square cavity, i.e. Xc=Yc. In the calculation of the magnetic current $\vec{M}$ by the MoM, the slot is equally divided into small segments $\Delta L (= \lambda_0/20)$. The center frequency f_0 in this chapter is the frequency where the axial ratio (AR) is minimum.

4.3.1 Conditions for Circular Polarization

Figure 4.2 shows the AR against a short-circuiting position Ls at $f_0 = 1.51$GHz. From this figure, we can see that the AR varies greatly with the short-circuiting position. This implies that the magnetic current distribution is strongly affected by the short-circuiting points.

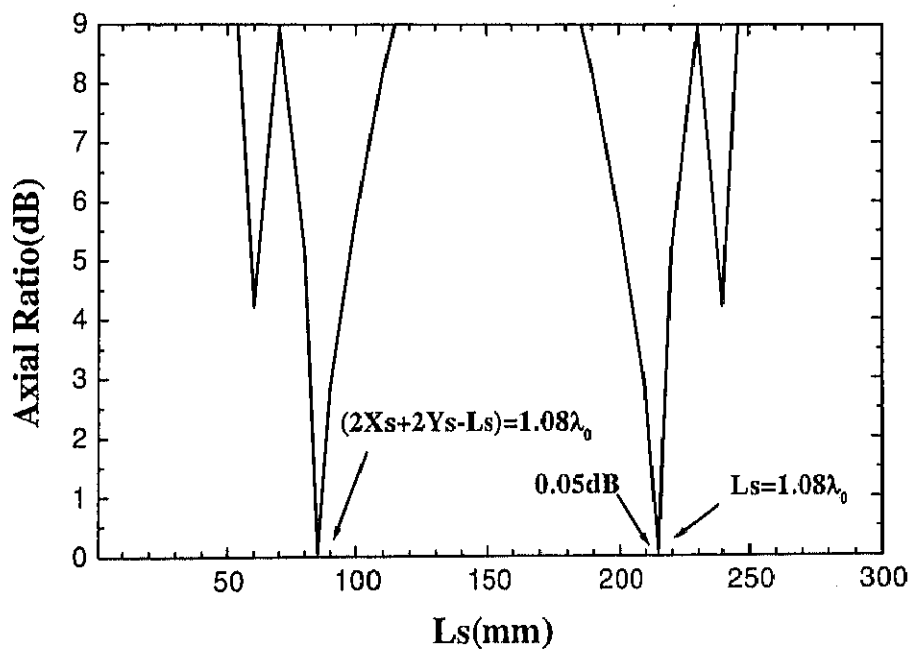

Fig. 4.2: Axial ratio against Ls, where Xc=Yc=160mm, Zc=22mm, Xs=50mm, Ys=100mm, Dx=19mm, W=4mm, f_0=1.51GHz.

When the short-circuiting points are set at $Ls = 1.08\lambda_0$ or $2Xs + 2Ys - 1.08\lambda_0 = 85$ mm, the AR reaches to its lowest value of 0.05dB. Note that the

two short-circuiting points are always symmetrical to the feed point and the senses of the polarization for the two short-circuiting points are opposite.

Figure 4.3 shows the magnetic current distribution on the slot where the amplitude of the magnetic current is normalized to the amplitude of the magnetic current at the feed point. The magnetic current amplitude and phase at f_0 represents a symmetrical traveling wave magnetic current distribution. The magnetic current with the linearly decreasing phase along the slot (points a $\rightarrow$ e $\rightarrow$ d $\rightarrow$ c and points g $\rightarrow$ h $\rightarrow$ i $\rightarrow$ j) generates circularly polarized waves. This magnetic current distribution is expected to give better radiation pattern characteristics than that of the single rectangular loop slot structure.

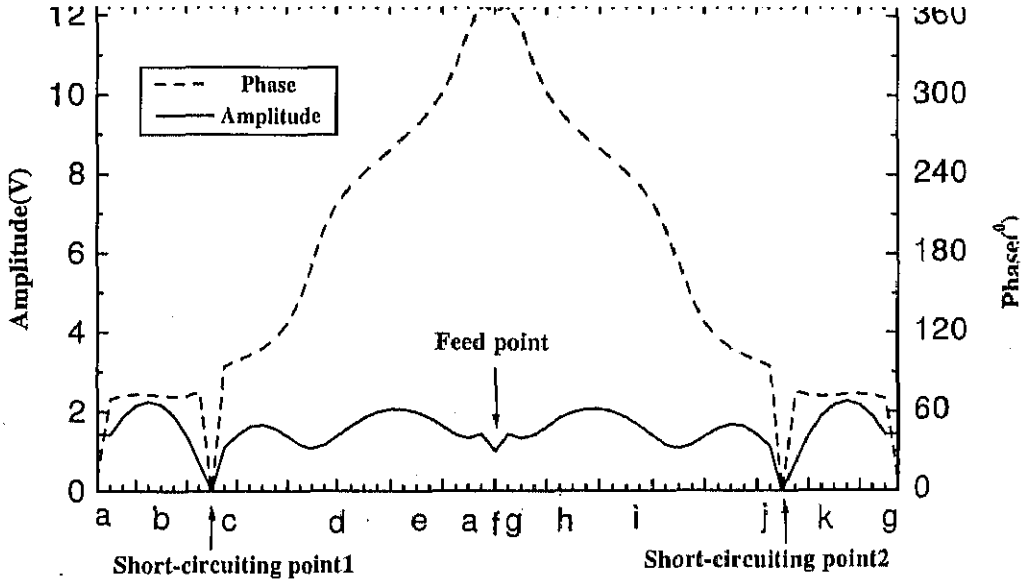

Fig. 4.3: Magnetic current distribution, where Xc=Yc=160mm, Zc=22mm, Xs=50mm, Ys=100mm, Dx=19mm, W=4mm, Ls=85mm, f_0=1.51GHz.

4.3.2 Input Impedance, VSWR and Axial Ratio Characteristics

Figures 4.4, 4.5 and 4.6 show the input impedance, VSWR and AR for different Zc (the depth of the cavity), respectively.

Figure 4.4 shows that the resonance frequency, where the input reactance is zero, is almost independent of Zc. From Fig. 4.5, it is seen that the VSWR minimum doesn't move with the change of Zc and the bandwidth of VSWR becomes slightly wider with the increase of Zc. For comparison, the AR for the antenna without a cavity is also plotted in Fig. 4.6. Note that there is a center frequency difference between the antenna without the cavity and the cavity-backed antenna. In Fig. 4.6, when the slot is backed by the cavity, the f_0 shifts to its higher end. Figure 4.6 displays that the center frequency decreases greatly with the increase of Zc. The bandwidth of AR ($\leq$3dB) remains constant and is about 8%. The lowest AR minimum for the five different Zc is 0.05dB when Zc=22mm=0.11λ_0. When Zc increases from 22mm to 28mm, the AR minimum is almost unchanged, whereas with the decrease of Zc from 22mm to 16mm, the AR minimum becomes high and reaches 1dB.

Figure 4.7 shows the f_0(center frequency), f_r(resonance frequency) and AR_{f_0}(AR at f_0) versus Xc (the width of the cavity). From Fig. 4.7, we can see that the resonance frequency is almost independent of Xc and the center frequency decreases with the increase of Xc just like the case for Zc. When Xc increases from 140mm to 160mm, the AR_{f_0} becomes lower and reaches the lowest value at Xc=160mm=0.8λ_0, whereas with the increase of Xc from 160mm to 180mm, the AR_{f_0} becomes higher quickly.

Figures 4.8, 4.9 and 4.10 show the input impedance, VSWR and AR for different Dx (the distance between the two rectangular loop slots), respectively. With the increase of Dx, the resonance frequency decreases, and the resistance also decreases at the resonance frequency, as shown in Fig. 4.8. This means that by adjusting Dx, the input impedance at the resonance can be controlled. Figures 4.9 and 4.10 demonstrate that the VSWR and the AR are insensitive to Dx.

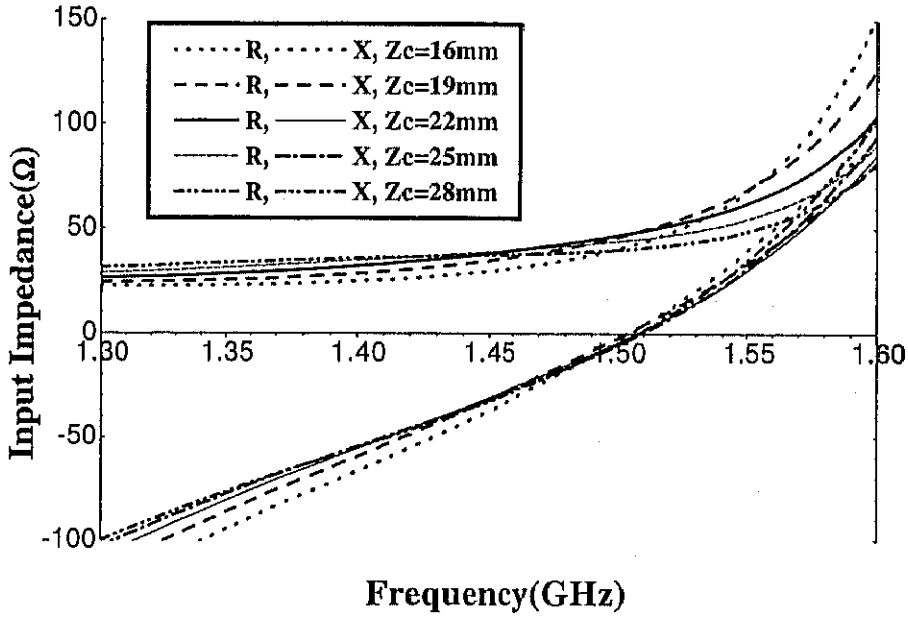

Fig. 4.4: Input impedance for different Zc, where Xc=Yc=160mm, Xs=50mm, Ys=100mm, Dx=19mm, W=4mm, Ls=85mm.

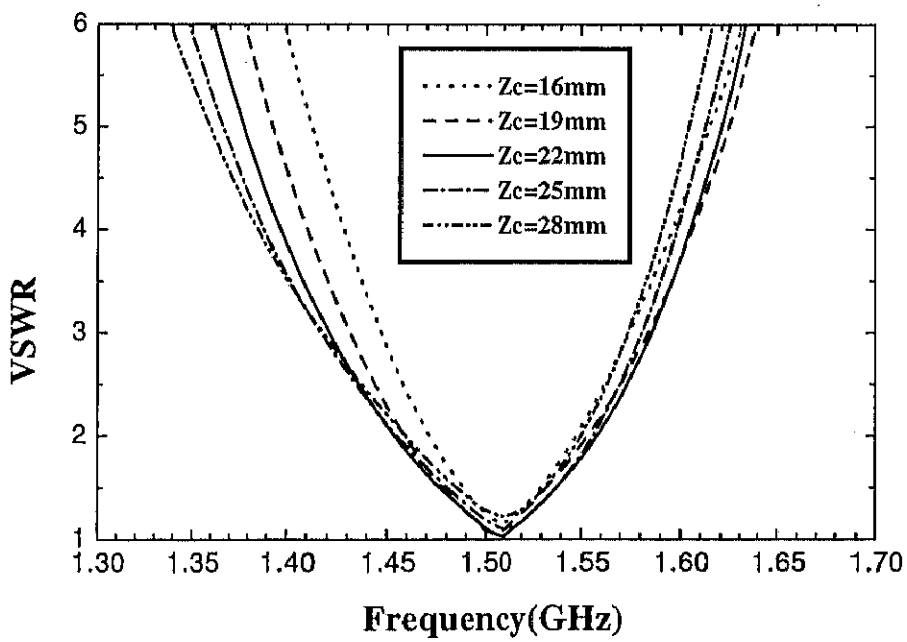

Fig. 4.5: VSWR for different Zc, where Xc=Yc=160mm, Xs=50mm, Ys=100mm, Dx=19mm, W=4mm, Ls=85mm.

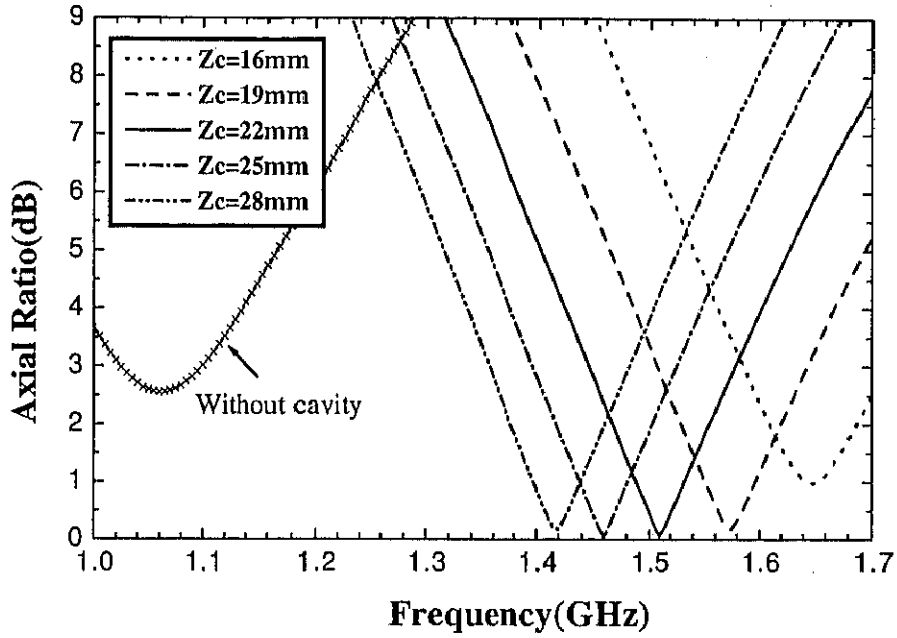

Fig. 4.6: Axial ratio for different Zc, where Xc=Yc=160mm, Xs=50mm, Ys=100mm, Dx=19mm, W=4mm, Ls=85mm.

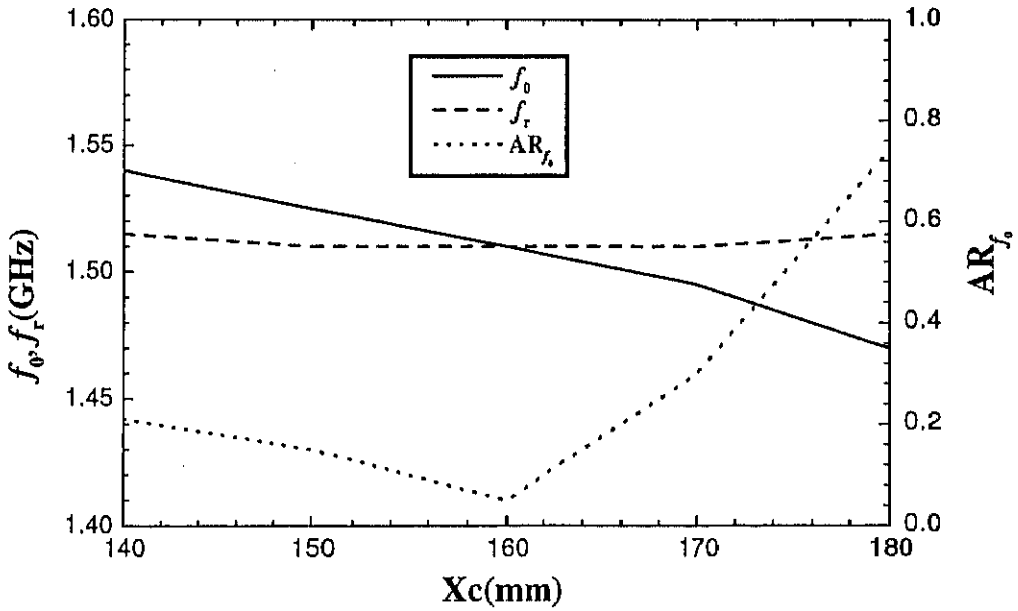

Fig. 4.7: f_0, f_r and AR_{f_0} versus Xc, where Zc=22mm, Xs=50mm, Ys=100mm, Dx=19mm, W=4mm, Ls=85mm.

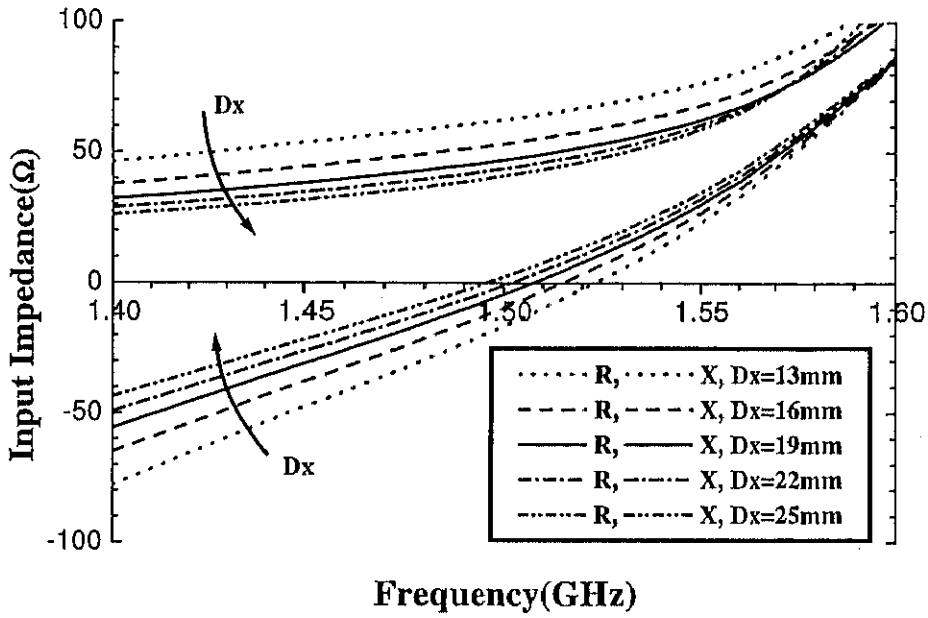

Fig. 4.8: Input impedance for different Dx, where Xc=Yc=160mm, Zc=22mm, Xs=50mm, Ys=100mm, W=4mm, Ls=85mm.

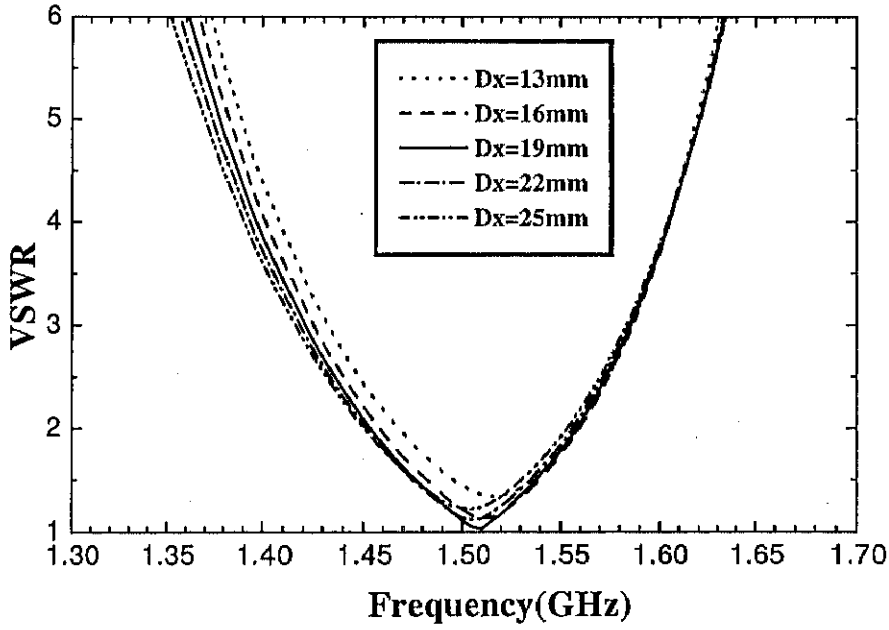

Fig. 4.9: VSWR for different Dx, where Xc=Yc=160mm, Zc=22mm, Xs=50mm, Ys=100mm, W=4mm, Ls=85mm.

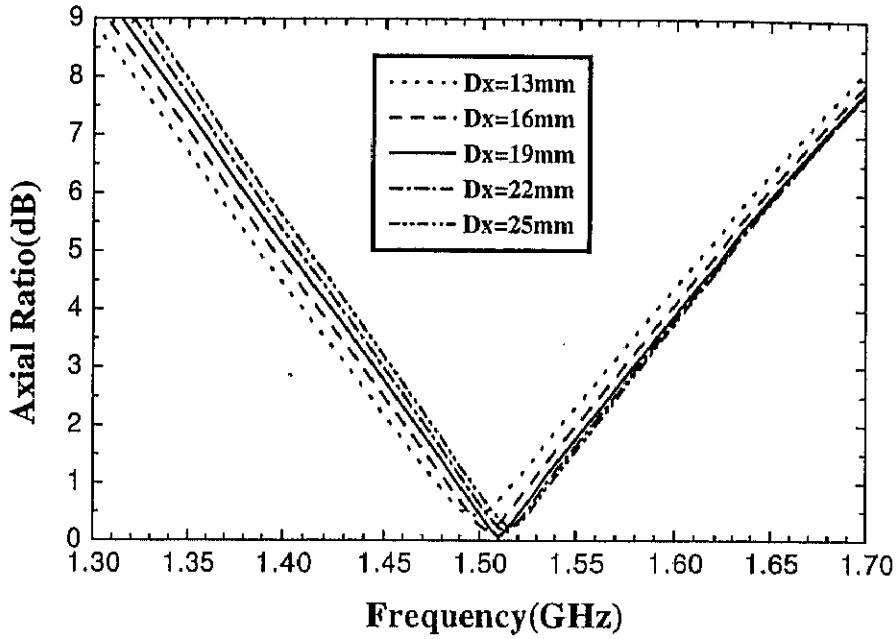

Fig. 4.10: Axial ratio for different Dx, where Xc=Yc=160mm, Zc=22mm, Xs=50mm, Ys=100mm, W=4mm, Ls=85mm.

4.3.3 The Bandwidth of VSWR and Axial Ratio

The VSWR and AR for different Xs/Ys (the ratio of the two side lengths of the rectangular loop slot) are shown in Figs. 4.11 and 4.12, respectively. For different Xs/Ys, the perimeter of the rectangular loop slot, i.e. 2Xs+2Ys, is kept 300mm. The parameters are optimized that the AR minimum and the VSWR minimum are at the same frequency for all of the Xs/Ys. When Xs/Ys increases from 0.36 to 0.67, the VSWR bandwidth ($\leq$2) increases from 4.3% to 10.8%, whereas the AR bandwidth ($\leq$3dB) decreases from 11% to 5.9%.

From the data in Figs. 4.11 and 4.12, we can get the relation between the VSWR bandwidth ($\leq$2) and the AR bandwidth ($\leq$3dB) as shown in Fig. 4.13. We can see from this figure that when Xs/Ys=0.528, the VSWR bandwidth and the AR bandwidth are the same and is 7.6%.

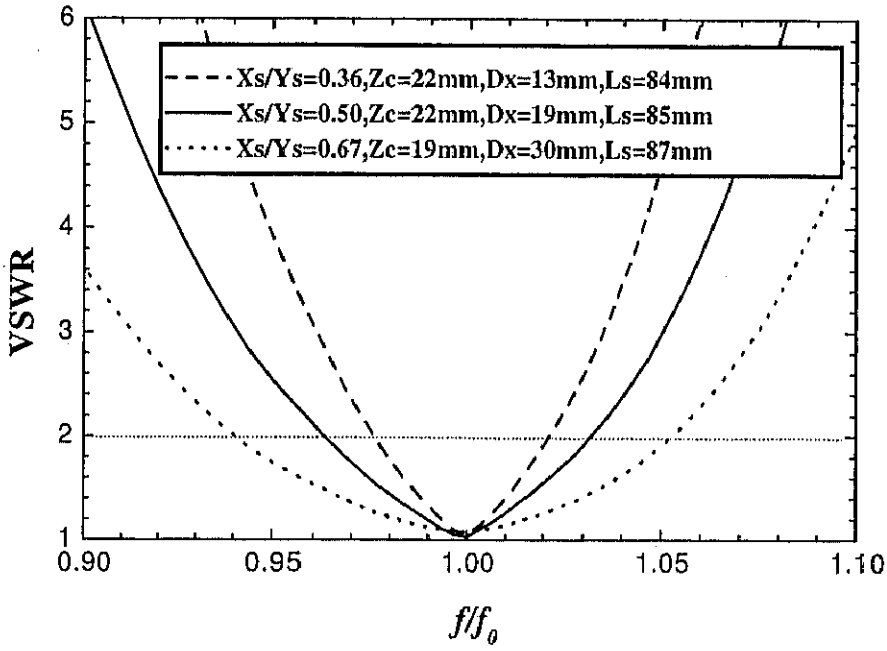

Fig. 4.11: VSWR for different Xs/Ys, where Xc=Yc=160mm, Xs+Ys=150mm, W=4mm.

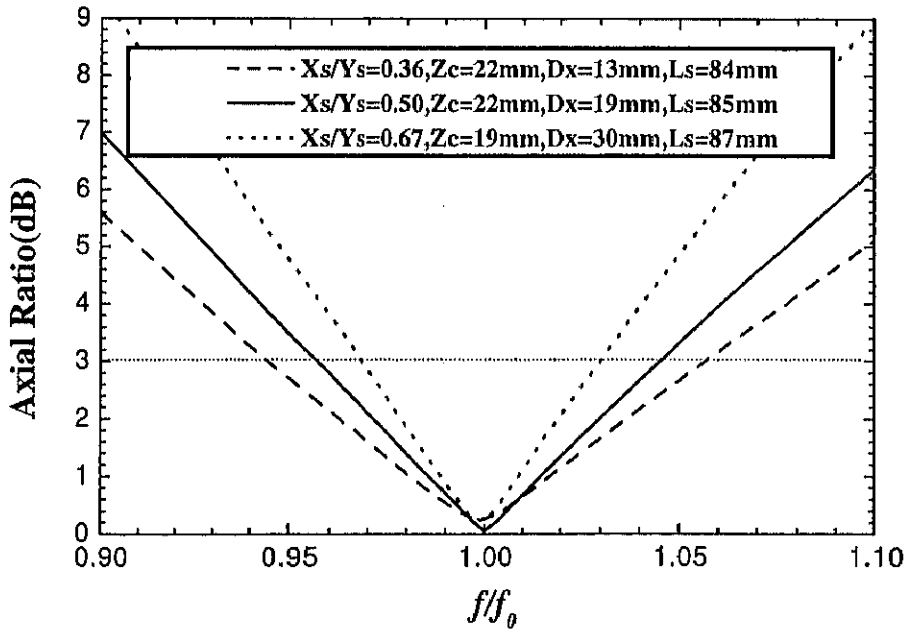

Fig. 4.12: Axial ratio for different Xs/Ys, where Xc=Yc=160mm, Xs+Ys=150mm, W=4mm.

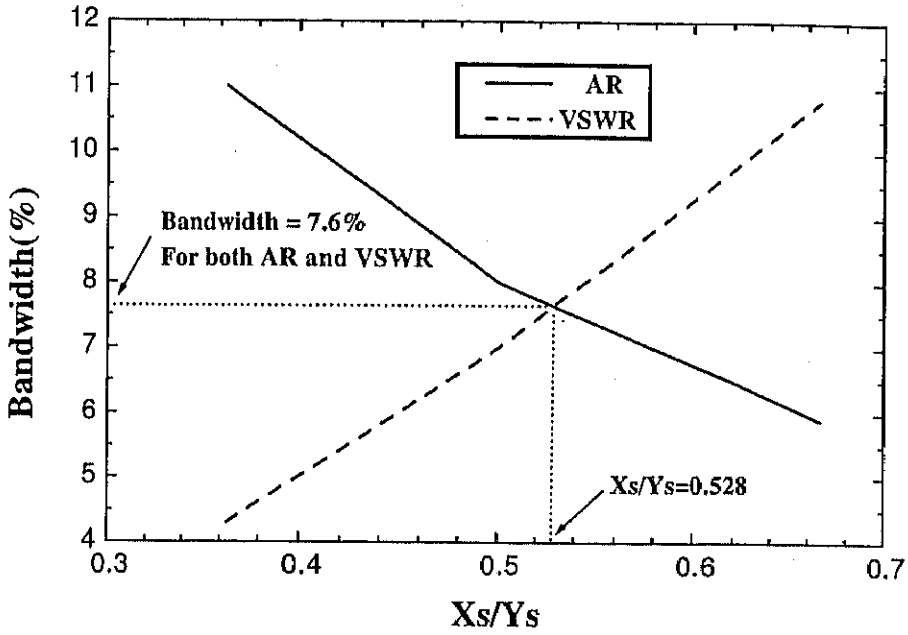

Fig. 4.13: The bandwidth of axial ratio and VSWR versus Xs/Ys.

4.3.4 Axial Ratio in a Constant ϕ Plane

Figure 4.14 gives the AR with respect to θ in $\phi = 0°, 45°, 90°$ and $135°$ planes, respectively. The AR's with respect to θ are symmetric to the z-axis and are similar in the different ϕ planes. The AR's are less than 3dB for $-40° \leq \theta \leq 40°$.

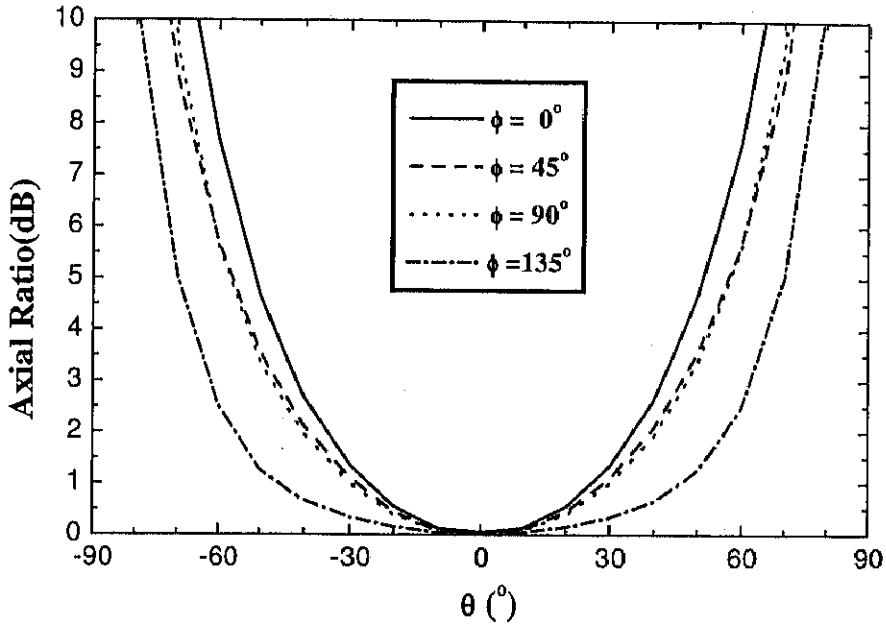

Fig. 4.14: Axial ratio with respect to in a constant plane at f_0=1.51GHz, where Xc=Yc=160mm, Zc=22mm, Xs=50mm, Ys=100mm, Dx=19mm, W=4mm, Ls=85mm.

4.4 Experimental Results

To validate the analysis, the experiment is performed. According to the discussion in the last section, the antenna dimensions are chosen as shown in Table 4.1. With these dimensions, the antenna is expected to radiate the optimized circularly polarized waves as calculated in the last section.

Xc	Yc	Zc	Xs	Ys	Dx	W	Ls
160mm	160mm	22mm	50mm	100mm	19mm	3mm	85mm

Table 4.1: Experimental dimensions of the rectangular-cavity-backed two-element rectangular loop slot antenna.

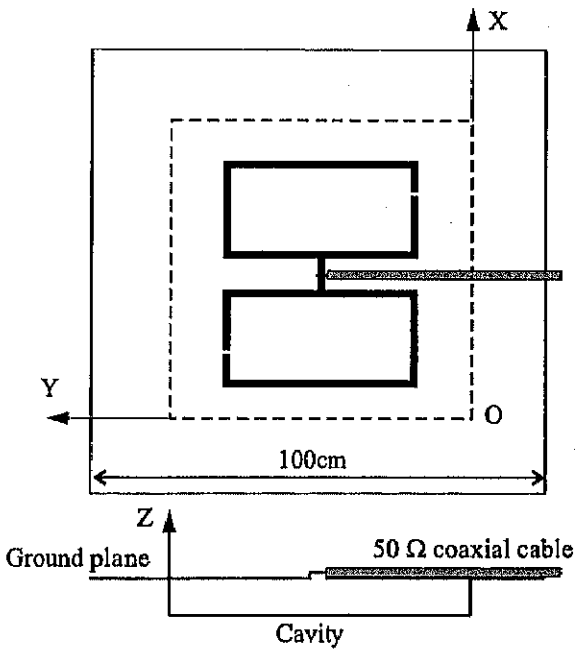

Fig. 4.15: Antenna structure in the experiment.

The antenna structure is shown in Fig. 4.15, where the antenna parameters and the way of feeding the slot by a 50 Ω coaxial cable are shown. In the experiment, a square copper plate of side 100cm and thickness 0.3mm is used as a ground plane. The two-element rectangular loop slot is formed on

the ground plane. The cavity is also made by the cooper plate of thickness 0.3mm. The slot is shorted with two cooper sheets of width 1mm. The slot is fed by a semi-rigid coaxial cable along the ground plane to minimize the effect of the feed line.

The computed and measured input impedance, AR and VSWR are shown in Figs. 4.16 and 4.17, respectively. The dimensions are optimized that the AR minimum and the VSWR minimum are at the same frequency. The VSWR minimum is adjusted to 1.01 to ensure the minimum reflection and the VSWR bandwidth of 7% is obtained. The AR minimum reaches as low as 0.05dB to realize the best circular polarization and the AR bandwidth reaches 8%. From Figs. 4.16 and 4.17, we can see that the computed input impedance, AR and VSWR are in good agreement with the measured results.

Figure 4.18 gives the computed and measured radiation patterns with respect to θ in $\phi = 0°$ and $90°$ planes, respectively. Because of the symmetrical magnetic current distribution, the radiation patterns are symmetric in all of the ϕ planes. The E_ϕ components are similar in all of the ϕ planes. We can see from this figure that the measured and calculated results are in good agreement.

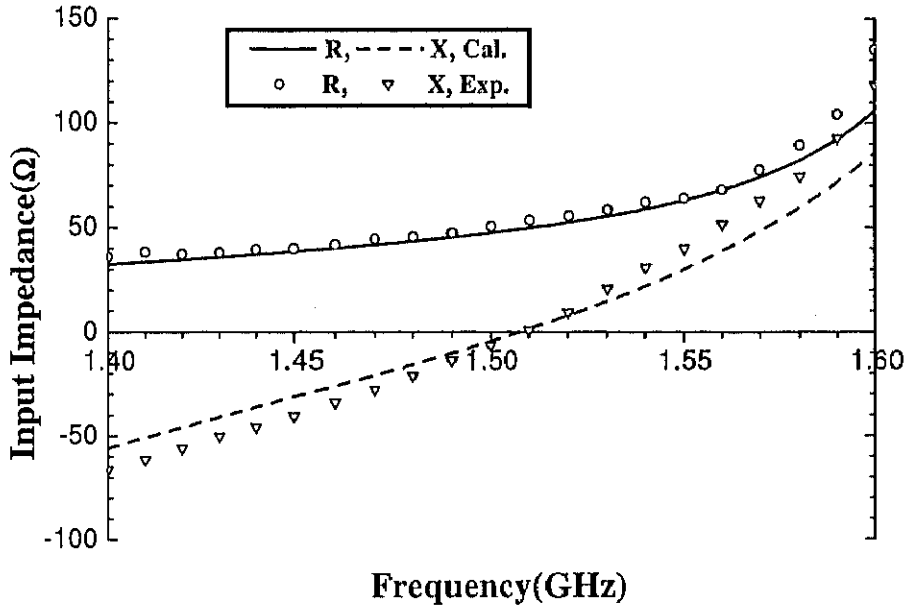

Fig. 4.16: Measured and calculated input impedance, where Xc=Yc=160mm, Zc=22mm, Xs=50mm, Ys=100mm, Dx=19mm, W=4mm, Ls=85mm.

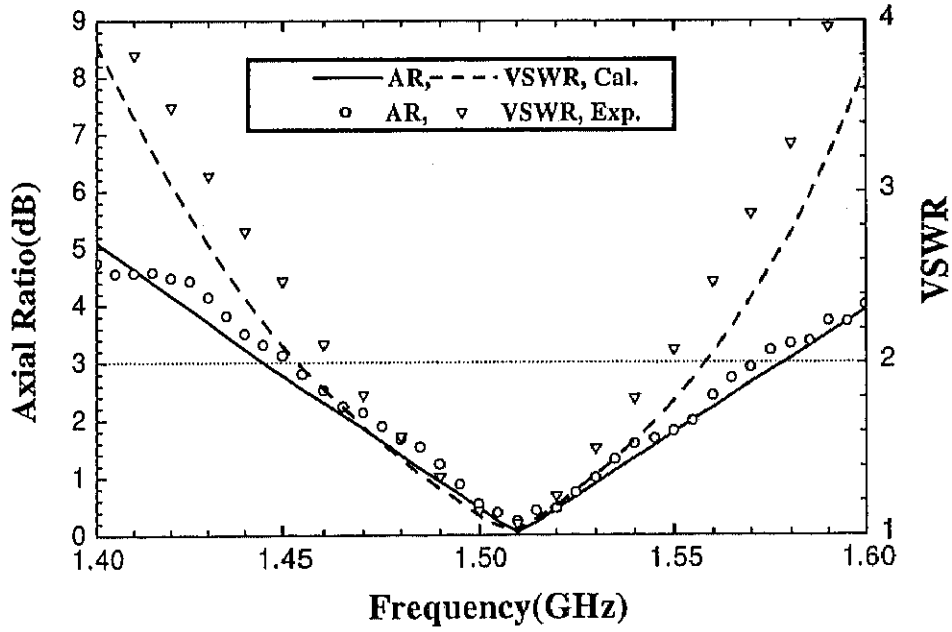

Fig. 4.17: Measured and calculated axial ratio and VSWR, where Xc=Yc=160mm, Zc=22mm, Xs=50mm, Ys=100mm, Dx=19mm, W=4mm, Ls=85mm.

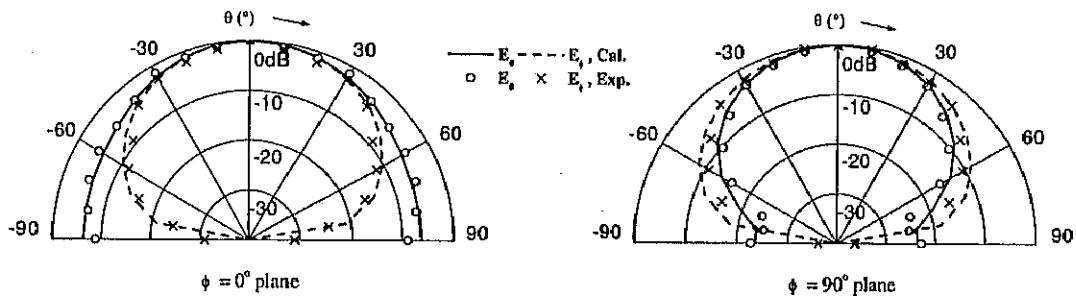

Fig. 4.18: Radiation patterns at f_0=1.51GHz, where Xc=Yc=160mm, Zc=22mm, Xs=50mm, Ys=100mm, Dx=19mm, W=4mm, Ls=85mm.

4.5 Conclusions

A rectangular-cavity-backed two-element rectangular loop slot antenna has been presented to radiate circularly polarized waves. The characteristics of the rectangular-cavity-backed two-element rectangular loop slot antenna are examined numerically and experimentally.

The circular polarization is realized by introducing two short-circuiting points across the slots. The axial ratio is very sensitive to the short-circuiting positions. When the short-circuiting points are put at $1.08\lambda_0$ from the feed point, the lowest AR of 0.05dB is obtained. The parameters of the antenna are optimized so that the AR minimum and the VSWR minimum are at the same frequency, and the VSWR minimum is adjusted to 1.01, to ensure the minimum reflection. The effect of the ratio of the two side lengths of the slot is significant on both the bandwidths of AR and VSWR. When the ratio is 0.528, the bandwidths of AR ($\leq$3dB) and VSWR ($\leq$2) become the same and reach 7.6%. The VSWR minimum is almost unchanged with respect to the width of the cavity and the depth of the cavity, whereas the center frequency is dependent on both the width and the depth of the cavity. By adjusting the distance between the two rectangular loop slots, the input impedance at the resonance can be readily controlled. The AR and VSWR are insensitive to the distance between the two rectangular loop slots. Because of the symmetrical magnetic current distribution, the radiation patterns are symmetric in all of the ϕ planes.

The calculated and experimental results on the input impedance, VSWR, AR and radiation pattern are in good agreement.